International Journal of Strategic Research in Education, Technology and Humanities
ISSN Print: 2465-731X | ISSN Online: 2467-818X

IJSRETH
Vol. 6, No. 1
January, 2019

Voltage Profile and Enhancement of Power Flow Using Steady-State Modeling of Static Synchronous Compensator and Thyristor Controlled Series Compensator

[1]Osuji, Christopher Uche & [2]Chukwulobe, Emmanuel E.
[1&2]Department of Electrical/Electronic Engineering,
Federal Polytechnic, Oko, Anambra State Nigeria

Abstract

Steady state-modelling of Static synchronous compensator and Thyristor controlled Series Compensator is modeled as a controllable voltage source in electrical power system that is in series with impedance and firing angle model for Thyristor controlled Series Compensator (TCSC) is used to control active power flow of the line to which TCSC is installed. Proposed model for TCSC takes firing angle as the state variable in the power flow formulation. To show the efficiency of the proposed models, Newton-Raphson method algorithm was implemented to solve the power flow equations in presence of Steady state-modelling of Static synchronous compensator (STATCOM) and TCSC. A 9-bus power system was used as a case study to demonstrate the performance of the proposed models. Simulation results show the effectiveness and robustness of the proposed models. Moreover, the power solution using the Newton-Raphson algorithm developed incorporating firing angle model possesses excellent convergence characteristics.

Keywords: *TCSC, STATCOM, Voltage Stability, Newton-Raphson*

Corresponding Author: Osuji, Christopher Uche

Background to the Study

The application of FACTS devices in operating power systems has been growing. However, achieving the full advantages of these devices is severely dependent on their type, size, number and their location. Furthermore, their optimal size and placement are affected by their steady state models applied in power system studies. But the use of exact model of FACTS devices in steady state calculations is complex, due to their switching behavior. On the other hand, applying very simple models such as pure inductor/capacitor for FACTS devices leads to inaccurate results. In addition, in a power market the use of inaccurate models for power system components affects the electrical energy pricing system; while this is very crucial when FACTS devices are used for congestion management of the transmission systems.

As a result of the development in electric power system engineering, particularly in the increased use of transmission facilities due to higher industrial output and deregulation, it is important to explore new ways of maximizing electric power transfer in existing transmission facilities, at the same time maintaining the acceptable levels of the network reliability and stability [3]. On the other hand, the fast development of power electronic technology has made FACTS (flexible AC Transmission system) promising solution of future power system. FACTS controllers such as Static Synchronous Compensator (STATCOM), Static VAR Compensator (SVC), Thyristor Control Series Compensator (TCSC), etc. are able to change the network parameters in a fast and effective way in order to achieve better system performance [4, 5]. These controllers are used for enhancing dynamic performance of power systems in terms of voltage/angle stability while improving the power transfer capability and voltage profile in steady state [6]

Static Synchronous Compensators (STATCOM) and Thyristor-Controlled Series Capacitor (TCSC) are members of flexible AC Transmission system family that have successfully been used in power systems to enhance both the steady state and dynamic performance of the systems. Static Synchronous Compensator compensate the reactive power from or to the power system. This function is identical to the synchronous condenser with rotating mass, but its response time is extremely faster than that of the synchronous condenser. This rapidity is very effective to increase transient stability, enhance voltage support and to damp low frequency oscillation for power transmission system [1].

Thyristor-Controlled Series Capacitor is an important component of FACTS. With the firing control of the thyristors, it can change its apparent reactance smoothly and rapidly. The TCSC is able to directly schedule the real power flow through a typically selected line and allow the system to operate closer to the line limits. More importantly because of its rapid and flexible regulation ability, it can improve transient stability and dynamic performance of the power systems. Particularly, in systems with large bulk transfer of power and long transmission lines it can be used to increase the power transfer capability and damp low frequency oscillations [5,7].

Now, for maximum utilization of any FACTS device in power system planning, operation and control, power flow solution of the network that contains any of these devices is a fundamental requirement, As a result, many excellent research studies have been carried out in the literature for developing efficient load flow algorithm for FACTS devices [3] This research focuses on the development of STATCOM and TCSC models and their implementation in Newton-Raphson load flow algorithm, to control voltage of the bus and active power across the line.

Load flow problem, Load Flow Equation
involves solving the set of non-linear algebraic equations which represent the network under steady state conditions [3]. The reliable solution of real life transmission and distribution networks is not a trivial matter and Newton-type methods, with their strong convergence characteristics, have proved most successful [2]. To show the power flow equations, the power flow across the general two-port network element connecting buses k and m shown in figure 1.1is considered and the following equations are obtained.

The injected active and reactive power at bus –k(P_k and Q_k) is:

$$P_k = G_{kk}V_k^2 + (G_{km}\cos\delta_{km} + B_{km}\sin\delta_{km})V_kV_m \quad 1$$
$$Q_k = -B_{kk}V_k^2 + (G_{km}\sin\delta_{km} - \cos\delta_{km})V_kV_m \quad 2$$
$$P_k = G_{mm}V_m^2 + (G_{mk}\cos\delta_{mk} + B_{mk}\sin\delta_{mk})V_kV_m \quad 3$$
$$Q_k = -B_{mm}V_m^2 + (G_{mk}\sin\delta_{mk} - \cos\delta_{mk})V_kV_m \quad 4$$

Note that: $\delta_{km} = \delta_k - \delta_m = -\delta_m$

$$Y_{kk} = Y_{mm} = G_{kk} + jB_{kk} = Y_{ko} + Y_{km}$$
$$Y_{km} = Y_{mk} = G_{km} + jB_{km} = -Y_{mk}$$

The nodal power flow equations are:

$$P = f(V,\theta,G,B);\ Q = g(V,\theta,G,B) \quad 5$$

Their linearisation around a base point (P^o, Q^o) is:

$$\begin{bmatrix}\Delta P\\ \Delta Q\end{bmatrix}^i = [J]^i \begin{bmatrix}\Delta\theta\\ \Delta V\end{bmatrix}^i \quad 6$$

P and Q are vectors of real and reactive nodal power injections as a function of nodal voltage magnitudes V and angles θ and network conductances G and susceptance B [5].

$\Delta P = P_{spec} - P_{cal}$ is the real power mismatch vector and $\Delta Q = Q_{spec} - Q_{cal}$ is the reactive power mismatch [10]. Vector $\Delta\theta$ and ΔV are the vectors of incremental changes in nodal voltage magnitudes and angles. J is the matrix of partial derivatives of real and reactive powers with respect to voltage magnitudes and angles and i indicates the iteration number.

Installation of FACTS devices in an existing load flow algorithm results in increased complexity of programming as a result of:

I. Existence of new terms owing to the contributions from the FACTS devices need to be included in the existing power flow equations of the concerned buses. These terms necessitate modification of existing power flow codes.
ii. New power flow equations related to the FACTS devices come into the picture, which dictate formulation of separate subroutine(s) for computing them.
iii. The system Jacobian matrix contains entirely new Jacobian sub-blocks exclusively related to the FACTS devices. Therefore, new codes have to be written for computation of these Jacobian sub-blocks [10]

iv. Increase in the dimension of the Jacobian matrix compared with the case when there are no power system controllers is proportional to the number and kind of such controllers. The simultaneous equations for the network and power system state variables are [8]:

$$f(X_{nsv}, R_{pscv}) = 0 \qquad 7$$
$$g(X_{nsv}, R_{pscv}) = 0 \qquad 8$$

$X_{n\delta v}$ is the Network state variables i.e., (voltage magnitudes and phase angles) and $R_{p\delta cv}$ is the Power system controller variables. The modified Jacobian incorporated FACTS controller structure is shown in figure 1 below.

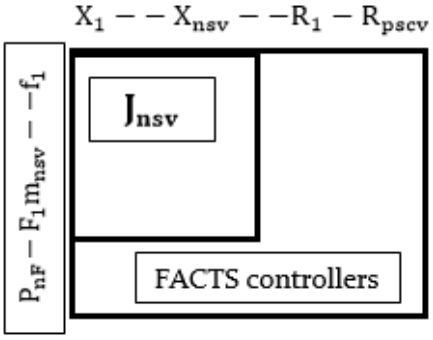

Figure 1: Modified Jacobian incorporated FACTS controllers.
Source: [5]

Statcom Incoporated Power System

The circuit model of a STATCOM connected to Bus k of an N-Bus power is shown in figure 1.3. The STATCOM is modeled as a controllable voltage source (E_{stat}) in series with impedance [11]. The real part of this impedance represents the Ohmic losses of the power electronic devices and the coupling transformer while the imaginary part of this impedance represents the leakage reactance of the coupling transformer. Assuming that the STATCOM is operating in voltage control mode, this means that the STATCOM absorbs proper amount of reactive power from the power system to keep $|V_k|$ constant for all power system loading

$$P_k = P_{stat} + \sum_{j=1}^{N} |V_k||V_j||Y_{kj}| \cos(\delta_k - \delta_j - \delta_{kj}) \quad 9$$

$$Q_k = Q_{stat} + \sum_{j=1}^{N} |V_k||V_j||Y_{kj}| \sin(\delta_k - \delta_j - \delta_{kj}) \quad 10$$

$$P_{stat} = G_{stst}|V_k|^2 - |V_k||E_{stst}||Y_{stat}| \cos(\delta_k - \delta_{stst} - \theta_{stat}) \quad 11$$

$$Q_{stat} = B_{stst}|V_k|^2 - |V_k||E_{stst}||Y_{stat}| \sin(\delta_k - \delta_{stst} - \theta_{stat}) \quad 12$$

Where: $|E_{stst}|$, δ_{stat}, $|Y_{stst}|$ and θ_{stat} are shown in figure 2. Addition of STATCOM introduces two new variables $|E_{stst}|$ and δ_{stat}; however, $|V_k|$ is now known. Hence, one more equation is needed to solve the power flow problem. Equations 11 and 12 are obtained using the fact that the power consumed by the source E_{stat} (P_{Estat}) must be zero in steady state condition.

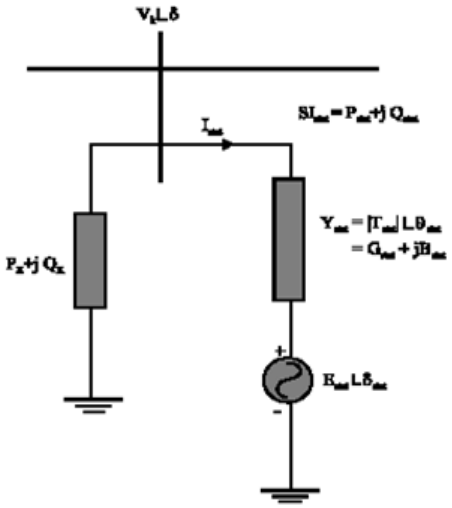

Figure 2: Steady state model of a STATCOM.
Source: [5]

Thus the equation for P_{Estat} is written as:

$$P_{E_{stst}} = \mathcal{R}l(E_{stat} I^*_{stat}) = -G_{stat}|E_{stat}|^2 + |E_{stat}||V_k||Y_{stat}| \cos(\delta_{stat} - \delta_k - \theta_{stat}) \quad 13$$

The power equation linearisation of STATCOM model is given as:

$$\begin{bmatrix} \Delta P_k \\ \Delta Q_k \\ \Delta P_{stat} \\ \Delta Q_{stat} \end{bmatrix} = \begin{bmatrix} \frac{\partial P_k}{\partial \theta_k} & \frac{\partial P_k}{\partial V_k} V_k & \frac{\partial P_k}{\partial \delta_{stat}} & \frac{\partial P_k}{\partial V_{stat}} V_{stat} \\ \frac{\partial Q_k}{\partial \theta_k} & \frac{\partial Q_k}{\partial V_k} V_k & \frac{\partial Q_k}{\partial \delta_{stat}} & \frac{\partial Q_k}{\partial V_{stat}} V_{stat} \\ \frac{\partial P_{stat}}{\partial \theta_k} & \frac{\partial P_{stat}}{\partial V_k} V_k & \frac{\partial P_{stat}}{\partial \delta_{stat}} & \frac{\partial P_{stat}}{\partial V_{stat}} V_{stat} \\ \frac{\partial Q_{stat}}{\partial \theta_k} & \frac{\partial Q_{stat}}{\partial V_k} V_k & \frac{\partial Q_{stat}}{\partial \delta_{stat}} & \frac{\partial Q_{stat}}{\partial V_{stat}} V_{stat} \end{bmatrix} \begin{bmatrix} \Delta \theta_k \\ \frac{\Delta V_k}{V_k} \\ \Delta \delta_{stat} \\ \frac{\Delta V_{stat}}{V_{stat}} \end{bmatrix} \quad 14$$

The voltage magnitude and phase angle are taken to be state variables.

Thyristor Controlled Series Compensator Model

Thyristor-Controlled Series Compensator (TCSC) allows rapid and continuous changes of transmission line impedance. Figure 3 shows the TCSC module connected in series with the transmission line. The structure of the controller is equivalent to the FC-TCR SVC [7]. However, the equivalent impedance of the TCSC at 50 Hz is more appropriately represented by assuming a sinusoidal steady-state total current rather than a sinusoidal voltage.

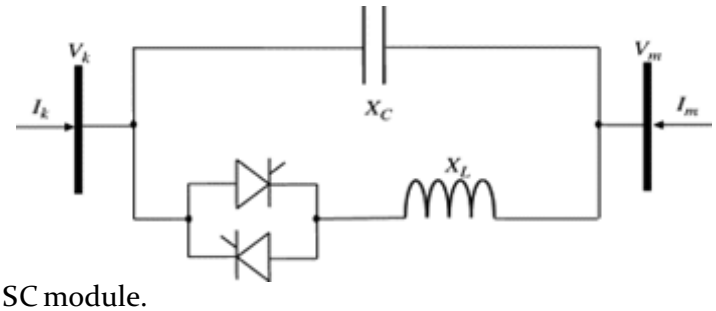

Figure 3: TCSC module.
Source: [6]

TCSC is represented by its fundamental frequency impedance in this work. The TCSC linearized power flow equations with respect to the firing angle are incorporated into an existing Newton-Raphson algorithm. Since the explicit information about the TCSC impedance-firing angle is available. Initial conditions are easily selected, hence preventing load flow iterative process from entering the non-operative regions owing to the presence of resonant bands. The fundamental TCSC equivalent reactance is given as:

$$X_{TCSC} = -X_C + K_1[2\sigma + \sin 2\sigma - K_2 cos^2\sigma(\omega \tan \omega\sigma)] \quad 15$$

Where: $\sigma = \pi - \alpha$

$$X_{LC} = \frac{X_C X_L}{X_C - X_L} \quad 16$$

$$K_1 = \frac{X_C + X_{LC}}{\pi} \quad 17$$

$$K_2 = \frac{(X_{LC})^2}{\pi X_L} \quad 18$$

The behavior of TCSC power flow model is influenced greatly by the number of resonant points which is given as:

$$\alpha = \pi\left[1 - \frac{(2n-1)\omega(\sqrt{LC})}{2}\right] \qquad 19$$

n = 1, 2, 3....

Note that near resonant point, a small variations in the firing angle will induce large changes in both X_{Tcsc} and $\partial X_{Tcsc}/\partial\alpha$. This in turn may lead to ill conditioned TCSC power equations.
To develop TCSC model, we assume that the transmission line admittance in which TCSC is connected is:

$$G_{TCSC} + jB_{TCSC} = \frac{1}{R+j(X+X_{TCSC})} \qquad 20$$

Power flow equations of the line k-m in which TCSC is placed is given by:

$$P_{km}^{TCSC} = V_k^2 G_{TCRC} - V_k V_m [G_{TCSC}\cos(\delta_{km})]] + B_{TCSC}\sin(\delta_{km}) \qquad 21$$

When TCSC is used to control power flow in the line k-m, the set of linearized power flow equations are given by:

$$\begin{bmatrix} \Delta P_k \\ \Delta P_m \\ \Delta Q_k \\ \Delta Q_m \\ \Delta P_{km}^{TCSC} \end{bmatrix} = \begin{bmatrix} \frac{\partial P_k}{\partial \theta_k} & \frac{\partial P_k}{\partial \theta_m} & \frac{\partial P_k}{\partial V_k}V_k & \frac{\partial P_k}{\partial V_m} & \frac{\partial P_k}{\partial \alpha} \\ \frac{\partial P_m}{\partial \theta_k} & \frac{\partial P_m}{\partial \theta_m} & \frac{\partial P_m}{\partial V_k}V_k & \frac{\partial |P_m}{\partial V_m} & \frac{\partial |P_m}{\partial \alpha} \\ \frac{\partial Q_K}{\partial \theta_k} & \frac{\partial Q_K}{\partial \theta_m} & \frac{\partial Q_K}{\partial V_k}V_k & \frac{\partial Q_k}{\partial V_m} & \frac{\partial Q_k}{\partial \alpha} \\ \frac{\partial Q_m}{\partial \theta_k} & \frac{\partial Q_m}{\partial \theta_m} & \frac{\partial Q_m}{\partial V_k}V_k & \frac{\partial |Q_m}{\partial V_m} & \frac{\partial Q_m}{\partial \alpha} \\ \frac{\partial P^{TCSC}}{\partial \theta_k} & \frac{\partial P^{TCSC}}{\partial \theta_m} & \frac{\partial P^{TCSC}}{\partial V_k} & \frac{\partial P^{TCSC}}{\partial V_m} & \frac{\partial P^{TCSC}}{\partial \alpha} \end{bmatrix} \begin{bmatrix} \Delta\theta_k \\ \Delta\theta_m \\ \frac{\Delta V_k}{V_k} \\ \frac{\partial V_m}{V_m} \\ \Delta\alpha \end{bmatrix} \qquad 22$$

The elements of additional row and column of the modified Jacobean can be written as:

$$\frac{\partial P_k}{\partial \alpha} = V_k V_m\left[-\frac{\partial G_{TCSC}}{\partial \alpha}\cos(\delta_{km}) - \frac{\partial B_{TCSC}}{\partial \alpha}\sin(\delta_{km})\right] \qquad 23$$

$$\frac{\partial Q_k}{\partial \alpha} = V_k V_m\left[-\frac{\partial G_{TCSC}}{\partial \alpha}\sin(\delta_{km}) - \frac{\partial B_{TCSC}}{\partial \alpha}\cos(\delta_{km})\right] \qquad 24$$

$$\frac{\partial G_{TCSC}}{\partial \alpha} = \frac{-2R(X+X_{TCSC})}{[R^2+(X+X_{TCSC})]^2}\frac{\partial X_{TCSC}}{\partial \alpha} \qquad 25$$

$$\frac{\partial B_{TCSC}}{\partial \alpha} = \frac{-1}{[R^2+(X+X_{TCSC})]^2}\frac{\partial X_{TCSC}}{\partial \alpha} + \frac{2\left(2(X+X_{TCSC})\right)^2}{[R^2+(X+X_{TCSC})]^2}\frac{\partial X_{TCSC}}{\partial \alpha} \qquad 26$$

$$\frac{\partial X_{TCSC}}{\partial \alpha} = -2C_1(1+\cos 2\alpha) + C_2\sin 2\alpha\{\omega\tan\left(\omega(\pi-\alpha)\right)\tan\alpha\} + C_2\left[m^2\frac{cos^3(\pi-\alpha)}{cos^3\{\omega(\pi-\alpha)\}}\right] \qquad 27$$

Also the elements of the added row in equation 21 can be written as:

$$\frac{\partial P_{km}^{TCSC}}{\partial \alpha} = V_k^2 \frac{\partial G_{TCRC}}{\partial \alpha} - V_k V_m \left[\frac{\partial G_{TCRC}}{\partial \alpha}\cos(\delta_{km}) + \frac{\partial B_{TCSC}}{\partial \alpha}\sin(\delta_{km})\right] \quad 28$$

$$\frac{\partial P_{km}}{\partial \delta_k} = -V_k V_m[-G_{TCRC}\sin(\delta_{km}) + B_{TCSC}\cos(\delta_{km})] \quad 29$$

$$\frac{\partial P_{km}^{TCSC}}{\partial \delta_m} = \frac{\partial P_{km}^{TCSC}}{\partial \delta_k} \quad 30$$

$$\frac{\partial P_{km}^{TCSC}}{\partial V_k} V_k = P_{km}^{TCSC} + V_k^2 G_{TCRC} \quad 31$$

$$\frac{\partial P_{km}^{TCSC}}{\partial V_m} V_m = P_{km}^{TCSC} - V_k^2 G_{TCRC} \quad 32$$

In the mismatch vector of equation 21, $\Delta P_{km}^{TCSC} = P_{km}^{Req} - P_{km}^{TCSC}$ is the active power flow mismatch for the TCSC module and P_{km}^{Req} is the required power flow in the TCSC branch. We can now solve for system variables along with the firing angle mismatch using equation 1.21, making use of modified Jacobean matrix. The firing angles is updated using the following equation;

$$\alpha^{i+1} = \alpha^i + \Delta\alpha \quad 32$$

$\Delta\alpha$ is the incremental change in the TCSC's firing angle and i shows ith iteration.

Simulation and Results

A 9-bus system is used to assess the effectiveness of STATCOM and TCSC models developed in this study. Figure 4 shows the single line diagram of system, with 230kV and 100MVA base has been considered [10]. Five cases are considered, STATCOM is connected at bus 8 and then at bus 5 and finally at bus 6, TCSC connected between line 7-8 and then between line 9-8.

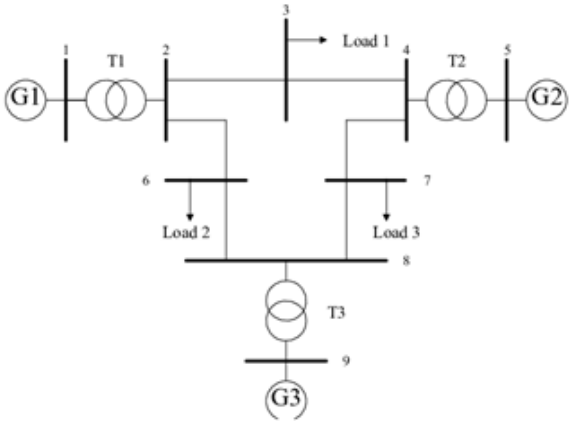

Figure 4: 9-bus system.
Source: [10]

Case A: STATCOM is connected to bus 8.
The control aim is to keep the voltage at that bus at 1.0 pu. The value X_{stat} is chosen as 0.14 pu. The convergent is obtained after 6 iterations. STATCOM absorbs 21.86 MAVR from bus 8 in order to keep the voltage magnitude at 1 pu, the associated values of E_{stat} and δ_{stat} are 0.9694 pu and 0.8268°, respectively. Table 1 shows the voltage magnitude and phase angle for all buses of the system with and without STATCOM

Case B: STATCOM is connected to bus 5.
The control aim is to keep the voltage at that bus at 1.0 pu. The value X_{stat} is chosen as 0.3 pu. The convergent is obtained after 6 iterations. STATCOM injects 4.84 MAVR in bus 8 in order to keep the voltage magnitude at 1 pu. The associated values of E_{stat} and δ_{stat} are 1.0145 pu and -3.989° respectively [11].

Case C: STATCOM is connected to bus 6.
To keep the voltage at bus 6 at 1.0 pu, the value X_{stat} is chosen as 0.2 pu. The convergent is obtained after 6 iterations. STATCOM absorbs 13.72 MAVR from bus 6 in order to keep the voltage magnitude at 1 pu, the associated values of E_{stat} and δ_{stat} are 0.9726 pu and -3.646°, respectively. The voltage magnitude and phase angle for all buses of the system are shown in table 1.

Table 1: The voltage magnitude and phase angle for all buses

	Bus								
Magnitude and angle	1	2	3	4	5	6	7	8	9
No facts									
V	1.0400	1.0250	1.0250	1.0258	0.9956	1.0127	1.0258	1.0159	1.0324
•	0.0000	9.2800	4.6648	-2.2168	-3.9888	-3.6874	3.7197	0.7275	1.9667
STATCOM at bus 8									
V	1.0400	1.0250	1.0250	1.0236	0.9916	1.0092	1.0189	1.0000	1.0269
•	0.0000	9.4248	4.7394	-2.2257	-3.9983	-3.6956	3.8269	0.8268	2.0270
STATCOM at bus 5									
V	1.0400	1.0250	1.0250	1.0274	1.0000	1.0140	1.0269	1.0167	1.0328
•	0.0000	9.2720	4.6722	-2.2121	-3.9886	-3.6762	3.7176	0.7339	1.9754
STATCOM at bus 6									
V	1.0400	1.0250	1.0250	1.0213	0.9920	1.0000	1.0243	1.0138	1.0295
•	0.0000	9.2759	4.6707	-2.2290	-4.0201	-3.6458	3.7077	0.7114	1.9650

Source: [11]

Case D: TCSC is connected between bus 7 and 8.
The control aim is to increase the real power flows in line 7-8 to 80 MW. The values of X_C and X_L are chosen as 9.522 Ω pu and 1.9 Ω with these values there is only one resonant point at α = 139.75°. Firing angle is set initially at 146° which lies on the capacitive region of TCSC. After running load flow program X_{tcsc} is equal to -0.0319 and the final firing angle value is 149.029°. Table 2 shows the power flow results of 9-bus system with and without TCSC and figure 1.6 the shows reactance-firing angle characteristics [10, 8]. From table 2, real power flow in line 7-8 at sending end increased from 76.38 to 80 MW.

Table 2: Power flow results of 9-bus system with and without TCSC. Source [11]

	Line	
Power flow results	7-8	9-8
Final firing angle value (°)	149.0300	149.2400
X_{tcsc} (pu)	-0.0319	-0.0439
Compensation (%)	-44.3000	-43.6000
Active power without TCSC (MW)	76.3800	24.1800
Active power with TCSC (MW)	80.0000	26.0000

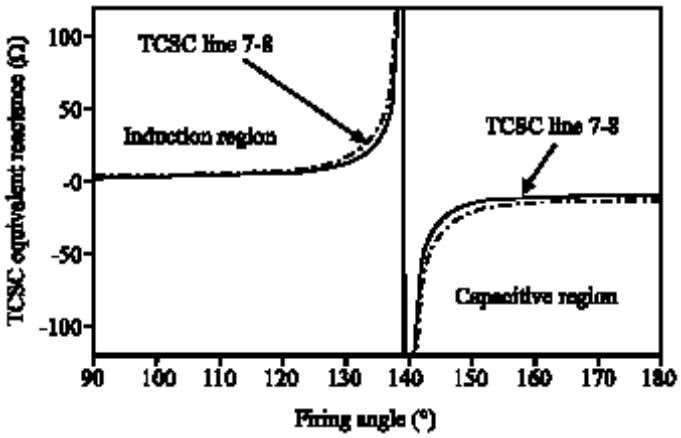

Figure 5: Reactance-firing angle characteristics

Case 5: TCSC is connected between bus 9 and 8, the control aim is to increase the real power flows in line 9-8 to 26 MW. The of values X_C and X_L are chosen as 13.33 Ω pu and 2.67 Ω with these values there is only one resonant point at α = 139.75°, firing angle is set initially at 146°, which lies on the capacitive region of TCSC. After running load flow program X_{tcsc} is equal to -0.0439 and the final firing angle value is 149.24°. The power flow results are tabulated as shown in table 2.Figure 5 shows reactance-firing angle characteristics [13]. From table 2, real power flow in line 9-8 at sending end increased from 76.38 to 80 MW.

Conclusion

In this study, steady-state models of STATCOM and TCSC for power flow solution were developed and discussed in details. STATCOM is modeled as a controllable voltage source in series with impedance where the voltage magnitude E_{stat} and phase angle δ_{stat} are taken to be state variables in power flow formulation, while firing angle model for TCSC is used to control active power flow of the line to which TCSC is installed. To demonstrate the effectiveness and robustness of the proposed models, a Newton-Raphson method incorporating firing angle model for STATCOM and TCSC was developed for desired power transferred and bus voltage profile improvement. Then the proposed models and algorithm were implemented on IEEE 9-bus system for different case studies. The results obtained show the effectiveness and robustness of the proposed models; moreover the power solution

using the Newton-Raphson algorithm developed incorporating firing angle model possesses excellent convergence characteristics.

References

Alammari, R., (1997). The voltage collapse problem based on the power system load ability, *Engineering Journal of University of Qatar, 10*,

Babulal, C. K., Kannan, P. S. & Maryanita, J. A (2006). Novel approach to determine static voltage stability limit and its improvement using TCSC and SVC, *Journal of Energy & Environment, 5*,

Boroujeni, H., Amani, M. & Abdollahi, M., (2012). Dynamic stability improvement by using STATCOM in a multi machine environment, *Research Journal of Applied Sciences, Engineering and Technology 4* (18) 3505-3509.

Bic, D. (2006). Static voltage stability analysis by participation factors computing, *Scientific Bulletin of the PetruMaior*, University of Targu Mures , p. 2.

Hemavathi, .C. R., (2012). Predication of voltage stability by using modal analysis, *National Conference on Electrical Science*s (NCES-12).

Kamarposhti, M . (2010). Evaluation of static synchronous compensator in order to loading margin study in power system, *Indian Journal of Science and Technology, 3* (5), 0974-6846. (May).

Palukuru, S. H. & Paul, S., (2010). Global voltage stability analysis of a power system using network equivalence technique in the presence of TCSC, *Leonardo Electronic Journal of Practices and Technologies, 16*

Sundarsingh, S., & Raja, R. P. (2012). Performance of thirty bus system with and without Statcom: International Conference on Trends in Electrical, *Electronics and Power Engineering*, 15-16,.

Shayanfar, A. H. A. & Rafiee, A., (2004). Impact of STATCOM and OPF on power system voltage stability using modal analysis and quadratic programming, Proceedings of The 12th Iranian *Electrical Engineering Conference, 1*, 25-29, Mashhad , May 11-13, Iran.

Tobaji1, E., Khaldi2, M. & Fadel, D., (2013). Statcom control of Ill-conditioned power systems using, *Advance in Electronic and Electric Engineering,* 3, (3), 311-320

Saad, M. S., & Edris, A., (2005). Delaying instability and voltage collapse in power systems using SVCs with washout filter-aided feedback, *American Control Conference, 8* (10)

Yonezawa, H., Tsukada, M. & Paserba, J., (2000). Study of a STATCOM application for voltage stability evaluated by dynamic PV curves and time simulations, *Power Engineering Society Winter Meeting, Conference, 2*, 23-27